A&A manuscript no.
(will be inserted by hand later)

Your thesaurus codes are:
06. (08.14.1; 02.04.1)

ASTRONOMY AND ASTROPHYSICS

Cooling neutron stars with localized protons

D.A. Baiko[1] and P. Haensel[2]

[1] A.F. Ioffe Physical Technical Institute, Politekhnicheskaya 26, 194021, St.Petersburg, Russia
e-mail: baiko@astro.ioffe.rssi.ru
[2] N. Copernicus Astronomical Center, Bartycka 18, 00-716, Warsaw, Poland
e-mail: haensel@camk.edu.pl

Accepted 20th January 2000

arXiv:astro-ph/0004185v1 13 Apr 2000

Abstract. We analyze cooling of neutron stars, assuming the presence of localized protons in the densest region of their cores. Choosing a single threshold density for proton localization and adjusting neutron star mass, we reproduce the observational data on effective surface temperatures of Vela and PSR 0656+14, with or without an accreted hydrogen envelope. However, the presence of a tiny hydrogen envelope is mandatory, in this model, for reproducing the Geminga data.

Key words: neutron stars–cooling–localized protons

The model of dense neutron star matter with localized protons was proposed by Kutschera & Wójcik (1993). According to these authors, in high-density matter with low proton fraction the "zero-point" (Fermi) kinetic energy of protons, estimated from the uncertainty principle, becomes small, compared to the energy of proton interactions with density waves of the neutron background. These density waves resemble hydrodynamic sound or long wavelength acoustic phonons in a solid. The coupling of protons to the neutron density waves results in a significant increase of proton effective mass in close analogy with polaron behaviour of a slow electron in a polar solid which also acquires a large effective mass because of the interactions with lattice phonons.

Moreover, considering one proton in neutron matter, Kutschera & Wójcik have shown that above some critical density $\rho_{\rm lp} \gtrsim 4\rho_0$ ($\rho_0 = 2.8 \times 10^{14}$ g cm^{-3}) the energy of a quantum state, in which a proton wave function is localized around some spatial point associated with the neutron density minimum, is lower than the energy of a state, where proton wave function is nonlocalized and the distribution of neutrons is uniform. Such a state also has an analog in solid state physics, the so-called small polaron state. It occurs when an electron interacts with a lattice so strongly that the latter deforms and this deformation traps the electron in a self-consistent manner.

This result by Kutschera & Wójcik may be applied to neutron star cores, where one has finite admixture of protons (rather than one proton in neutron matter), if the proton fraction x_p is so small that wave functions of neighbouring localized protons do not overlap. Small proton fractions in high density neutron-star matter were obtained by Wiringa et al. (1988), who performed extensive many-body calculations of the ground state, based on variational method and assuming realistic nuclear hamiltonian. In particular, their UV14+TNI model, which will be used further, predicts a proton fraction below 5% for densities $\rho > 3\rho_0$, and, eventually, complete disappearance of protons at about $7\rho_0$. This result is in contradiction with some other calculations of equation of state (EOS) of neutron star matter [based on the relativistic mean-field approach, see Glendenning (1996), or performed within the Brueckner-Bethe-Goldstone many-body theory, e.g., Baldo et al. (1997)] which yield a proton fraction growing monotonically with baryon density n_b. The high density behaviour of $x_p(n_b)$ is, therefore, subject to a significant theoretical uncertainty. Arguments in favor of $x_p(n_b)$, which decreases and eventually vanishes at high n_b, were presented by Kutschera (1994).

The localization of protons (if confirmed) leads to dramatic changes of basic kinetic properties of matter in the neutron star core. The reason is that the localized protons are very efficient scatterers of the main transport agents, electrons and neutrons. In effect, in the low-temperature regime, the thermal conductivity κ, for instance, behaves as $\propto T$, instead of the conventional T^{-1} dependence when scattering is provided by degenerate particles. As shown by Baiko & Haensel (1999) (hereafter Paper I), this extends the time scale of thermal equilibration in the neutron star core by about two orders of magnitude independently of the state of neutrons (normal or superfluid).

The neutrino emissivity of matter with localized protons is also very non-standard. First of all, the conventional beta-processes which involve charged currents (direct or modified Urca processes) are forbidden since at given baryon density the minimum of energy corresponds to a specific proton fraction, while any process which changes this fraction would require rearrangement of the whole state and, consequently, much larger energy

Send offprint requests to: P. Haensel

than the thermal energy available, say, at $T \lesssim 10^9$ K. Thus, the only possible processes are those which involve neutral currents. These are bremsstrahlung of neutrino–antineutrino pairs in nn, np, and ep collisions.

The kinetic properties of matter with localized protons were considered in Paper I. In particular, simple analytical formulae were derived for the electron and neutron thermal conductivities and shear viscosities, for the electron electrical conductivity as well as for the neutrino emissivity from np and ep bremsstrahlung. All these quantities were calculated under two simplifying assumptions. Firstly, it was assumed that the localized protons did not exibit any correlations (i.e., behaved like impurities). Secondly, the in-vacuum matrix elements of strong interactions were used. Both assumptions lead to an increase of the reaction rates by a factor of a few, since it is generally expected that the medium effects and correlation of scatterers reduce the matrix elements of elementary scattering processes, at least for small momentum transfers. Thus the results of Paper I give the upper bounds to the neutrino emissivities and the lower bounds to the transport coefficients. In other words, they represent the maximum effect that one can expect from the proton localization.

The aim of the present paper is to apply the results of Paper I to modelling neutron star cooling in order to check if the hypothetical proton localization is compatible with observational data on the neutron star effective surface temperatures. To do that we have to specify the neutron star model. In the core (at densities $\rho > \rho_{\rm cr} = 2.5 \times 10^{14}$ g cm^{-3}), we take the UV14+TNI EOS by Wiringa et al. (1988), while in the crust (below $\rho_{\rm cr}$) we take the EOS by Negele & Vautherin (1973) above neutron-drip density, and the EOS by Baym et al. (1971) below neutron-drip density. The model is then determined by the only parameter, the central mass density $\rho_{\rm c}$, and is constructed by integrating the Tolman-Oppenheimer-Volkoff equation outward the center.

We use the cooling code described, e.g., in Levenfish et al. (1999). The code includes explicitly effects of General Relativity (GR) and traces a steady thermal evolution of a spherically symmetric neutron star. Matter at densities $\rho > \rho_{\rm b} = 10^{10}$ g cm^{-3} is assumed to be isothermal with constant temperature $T_{\rm i}^{\infty}$ (as measured at infinity). The local temperature, $T_{\rm i}$, appears to be dependent on the radial coordinate r due to the GR effect. The cooling is governed by the thermal balance equation with energy losses due to neutrino emission from the core and photon emission from the stellar surface. The local effective surface temperature $T_{\rm s}$ is obtained from the local internal temperature, $T_{\rm b}$, at $\rho = \rho_{\rm b}$ using the formula by Potekhin et al. (1997). The latter formula fits the results of numerical simulations of heat transport through the crust. The formula depends also on the mass ΔM of the outer envelope made of light elements (light envelope). Such an envelope may, in principle, reside on the neutron star surface and due to its higher thermal conductivity the envelope would decrease the thermal insulation of the inner stellar regions and modify the $T_{\rm s}(T_{\rm b})$ relationship. The surface temperature $T_{\rm s}^{\infty}$, as measured by a distant observer, is related to $T_{\rm s}$ as $T_{\rm s}^{\infty} = T_{\rm s}\sqrt{1-2GM/Rc^2}$, where M and R are, respectively, the mass and radius of the neutron star.

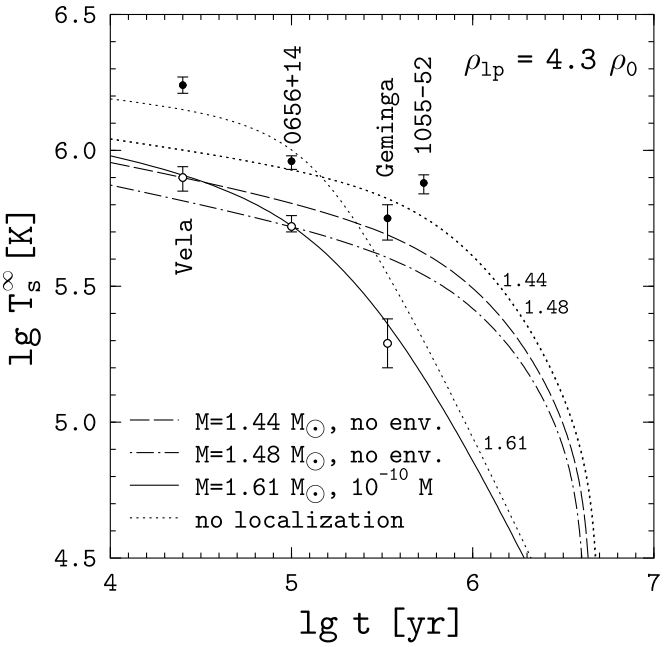

Fig. 1. Redshifted surface temperature versus neutron star age. Filled circles represent interpretation of observations with the black-body model while open circles are the "atmospheric" interpretations. The threshold parameters for proton localization are $x_{p0} = 5\%$ and $\rho_{\rm lp} = 4.3\rho_0$. The solid curve corresponds to the stellar model with an envelope of light elements, while the dashed and dot-dashed curves are calculated assuming no light envelope. The dotted curves are for the same star models (masses, presence or absence of the envelope) but without proton localization.

For our purposes we have introduced a number of modifications into the cooling code. All the changes are related to matter at densities above $\rho_{\rm lp}$. First of all, we have removed the proton contribution to the heat capacity. Then we have revised contributions to neutrino emissivity. Above $\rho_{\rm lp}$, if neutrons are nonsuperfluid (which is the case in study), the main contribution to the neutrino emissivity is due to nn and np neutrino-pair bremsstrahlung. The rate of the nn process is not changed by the proton localization, while the emissivity of the np process reads (Paper I):

$$Q_{\rm Brem}^{np} = 1.3\times10^{21}\left(\frac{n_b}{4n_0}\times\frac{x_p}{0.01}\right)\left(\frac{n_n}{4n_0}\right)^{4/3}\left(\frac{m_n^*}{m_n}\right)^2 \times S_{np}^{\rm t}\,T_9^6 \quad {\rm ergs\,s^{-1}\,cm^{-3}}, \qquad (1)$$

where x_p is the fraction of protons by number, n_n is the neutron number density, m_n and m_n^* are the bare and

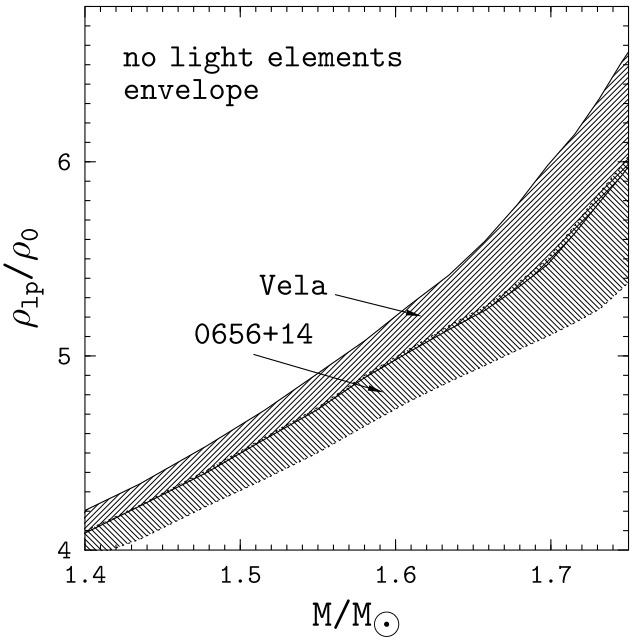

Fig. 2. Threshold density of localized protons versus mass of a neutron star for cooling model without envelope of light elements on the surface. The dotted and solid lines confine the parameter domains corresponding to the $T_{\rm s}^{\infty}$ error bars of PSR 0656+14 and Vela, respectively.

effective neutron masses, respectively; $n_0 = 0.16$ fm^{-3}, and T_9 is (local) temperature in units of 10^9 K. Finally, $S_{np}^{\rm t}$ is a function of n_n related to the total np cross-section in vacuum,

$$S_{np}^{\rm t} = 26.09 + 3.444\,\frac{4n_0}{n_n}. \qquad (2)$$

Typical cooling curves obtained within this model are presented in Fig. 1. The effect of the proton localization can be easily seen by comparing the dotted curves, which represent the cooling without the proton localization, with curves of other types, which show a faster cooling due to the localization effect. The rate of cooling without the proton localization is virtually independent of the mass: the dotted curves for 1.44 $M_\odot$ and 1.48 $M_\odot$ stars coincide. If the effect of the proton localization is taken into account, the more massive star cools more rapidly because at fixed threshold density, $\rho_{\rm lp}$, the more efficient neutrino pair bremsstrahlung in neutron-localized proton collisions is operative in a larger region of the neutron star core leading to a larger overall neutrino luminosity.

The results of our cooling simulations may be used for interpretation of thermal emission from the surface of cooling neutron stars of ages $t \gtrsim 10^4$ yr, which is the typical thermal equilibration time for neutron stars with localized protons (Paper I). At present there are 4 sources, identified as isolated neutron stars, which show thermal soft X-ray emission and have characteristic ages t in excess of 10^4 yrs. These are Vela, PSR 0656+14, Geminga and PSR 1055-52. The data that we use are summarized in Table 1. The effective surface temperatures $T_{\rm s}^{\infty}$ are determined from fitting the observed spectra of the sources in two different ways, either by black-body spectra ($T_{\rm bb}^{\infty}$ in Table 1) or by spectra obtained in realistic models of magnetized neutron star atmospheres (T_H^{∞} in Table 1 for magnetized hydrogen atmosphere). The inferred values of $T_{\rm s}^{\infty}$ appear to be quite different. Radiation emerging from an atmosphere composed of light elements (hydrogen and helium) has harder spectrum than the black-body radiation with the same $T_{\rm s}^{\infty}$ due to the decrease of opacity at higher energies (Romani 1987). Consequently, the effective temperatures predicted by the atmosphere models are 2-3 times lower than the black-body ones which require lower d/R (distance to radius) ratio. With the stellar radius fixed around the standard value of 10 km this translates into about 10 times smaller distances to the objects. The atmospheres composed of iron, on the contrary, produce radiation with a softer spectrum which is more similar on average to that of a black body.

The magnetic fields inferred from the spin-down rates are above 10^{12} G for all 4 stars. Such fields must have significant effect on the atmospheric opacities and therefore will modify the emerging spectrum (Shibanov et al. 1992). In general, the magnetic field makes the spectrum softer and somewhat elevates the effective temperature compared to the non-magnetized atmosphere case. However, no accurate magnetized atmosphere model have been developed so far for the relevant temperature range ($T_{\rm s} < 10^6$ K) where one should take into account effects of atom motion on the opacity (e.g., Pavlov & Zavlin, 1998).

	Vela	0656+14	Geminga	1055−52
$t, 10^4$ yrs	2.5[a)]	11	34	54
$T_{\rm bb}^{\infty}, 10^5$ K	17.4±1.2	9.1±0.5	$5.6^{+0.7}_{-0.9}$	7.5±0.6
$T_{\rm bb}^{\infty}$, Ref	[OFZ93]	[PMC96]	[HW97]	[OF93]
$T_H^{\infty}, 10^5$ K	7−8.6	$5.3^{+0.4}_{-0.3}$	2−3	–
T_H^{∞}, Ref	[PSZ96]	[ACPRT93]	[MPM94]	–

Table 1. The observational data on the 4 middle-aged isolated neutron stars.
[a)] according to Lyne et al. (1996);
[OFZ93] Ögelman et al. (1993);
[PMC96] Possenti et al. (1996), 90% confidence level (c.l.);
[HW97] Halpern & Wang (1997), 90% c.l.;
[OF93] Ögelman & Finley (1993);
[PSZ96] Page et al. (1996), 90% c.l., for adopted lower limit of distance $d = 300$ pc;
[ACPRT93] Anderson et al. (1993);
[MPM94] Meyer et al. (1994), typical value of the surface redshift factor, $T_{\rm s}^{\infty}/T_{\rm s} = 0.8$, were used.

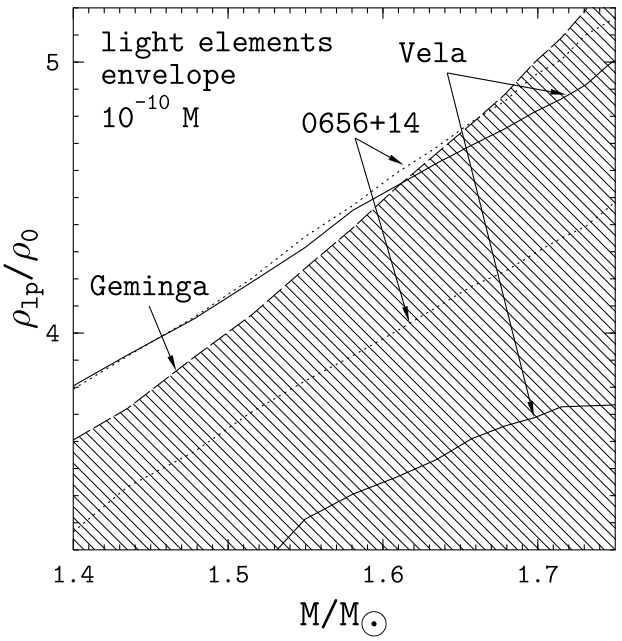

Fig. 3. Same as in Fig. 2 but for the model of a neutron star with envelope of light elements (of mass $10^{-10}\,M$) on the surface. The dashed line confines the (shaded) parameter domain allowed for Geminga.

These effects were neglected while obtaining the values reproduced in Table 1.

The surface temperatures $T_{\rm s}^{\infty}$ are plotted in Fig. 1. The filled and open circles correspond to black-body models and simplified magnetized hydrogen atmosphere models, respectively. As one concludes from Table 1 and the figure, the overall theoretical uncertainty in surface temperatures appears to be quite large; for instance $T_{\rm s}^{\infty} \sim (2{-}6) \times 10^5$ K for Geminga. This does not allow one to draw any definite conclusion about the cooling scenario of the neutron star except that it probably rejects the "rapid" cooling (via direct Urca process unsuppressed by superfluidity in dense matter). We note that the surface temperatures obtained from the hydrogen atmosphere models are rather low and cannot be explained within the "standard" cooling scenario (the neutrino losses via modified Urca process from non-superfluid matter). On the other hand, such a scenario can explain the black-body temperatures. Thus, the "atmospheric" temperatures (if the true temperatures turn out to be close to them) may provide more stringent test of the theory of neutron-star interior. For this reason let us adopt the "atmospheric" interpretation of observations and focus on lower error bars of Vela, PSR 0656+14, and Geminga.

Having fixed EOS we are left with three parameters which influence the cooling. These are the central stellar density $\rho_{\rm c}$ and the threshold values of mass density, $\rho_{\rm lp}$, and proton fraction, x_{p0}. In addition, we can vary ΔM, the mass of the surface envelope made of light elements. Note, that the presence of the hydrogen atmosphere is not equivalent to the presence of a light envelope as the amount of hydrogen needed to modify the emerging spectrum (1-10 g cm^{-2} or $\sim 10^{-20}{-}10^{-19}M_{\odot}$) is much lower than that required to change the $T_{\rm s}(T_{\rm b})$ relationship. Let us fix the threshold proton fraction $x_{p0} = 5\%$, and consider two models: without envelope, Fig. 2, and with a light envelope of mass $\Delta M = 10^{-10}M$, Fig. 3. The strips bounded by the lines of various types in Figs. 2 and 3 correspond to the domain of $\rho_{\rm lp}$ and M, for which cooling curves cross the error bar of a given source. Let us stress that Geminga (whose parameter domain is shaded in Fig. 3) can be explained only assuming the light envelope. In the latter case and for realistic $\rho_{\rm lp}$ (presumably above $4\rho_0$) the mass of Geminga should be above 1.5 $M_{\odot}$. The other two sources can be explained either with or without the envelope but for fixed $\rho_{\rm lp}$ their masses in the model with envelope should be higher. Finally let us mention that the strips are not very sensitive to the envelope mass for $\Delta M \gtrsim 10^{-10}M$.

Fig. 1 illustrates the cooling curves for the fixed threshold density $\rho_{\rm lp} = 4.3\rho_0$. The solid curve represents the model with the light envelope and $M = 1.61M_{\odot}$ ($\rho_{\rm c} = 5.4\rho_0$). It crosses the "atmospheric" error bars of Vela, PSR 0656+14 and Geminga simultaneously. The dashed and dot-dashed curves are envelope-free models. The masses should be lower, for instance, 1.44 and $1.48M_{\odot}$ for Vela and PSR 0656+14, respectively.

We have performed cooling simulations of neutron stars, with realistic equation of state, assuming localization of protons above some threshold density. These results have been used for interpretation of effective surface temperatures of observed isolated, middle-aged neutron stars ($t \geq 10^4$ yr). We have shown that the available observational data are consistent with the proton localization and can be reproduced if one chooses model parameters within the specific domains in the $\rho_{\rm lp} - M$ plane. Choosing a single threshold density for proton localization and adjusting neutron star mass, we reproduce the observational data for Vela and PSR 0656+14, with or without an accreted, hydrogen envelope. However, the presence of the hydrogen envelope is required in this model for explaining the observations of Geminga.

In conclusion, we note that the localization of protons is not necessary for the explanation of the available data on neutron star effective surface temperatures. Nevertheless, as is seen from the Fig. 1, it changes significantly the cooling rate and, if its existence is confirmed, it represents an important effect to be taken into account in realistic neutron star cooling calculations.

Acknowledgements. We are grateful to D.G. Yakovlev and Yu.A. Shibanov for enlightening discussions. Special thanks go to K.P. Levenfish and O.Yu. Gnedin for assistance with the cooling code. The work was supported in part by RFBR (grant 99-02-18099), INTAS (96-0542), and KBN (2 P03D 014 13).

References

Anderson S. B., Córdova F. A., Pavlov G. G., Robinson C. R., Thompson R. J., Jr., 1993, ApJ, 414, 867
Baiko D. A., Haensel P., 1999, Acta Physica Polonica, B30, 1097; astro-ph/9906312; Paper I
Baldo M., Bombaci I., Burgio G. F., 1997, A&A, 328, 274
Baym G., Pethick C., Sutherland P., 1971, ApJ, 170, 299
Glendenning, N. K., 1996, Compact Stars, Springer, New York
Halpern J. P., Wang F. Y.-H., 1997, ApJ, 477, 905
Kutschera M., Wójcik W., 1993, Phys. Rev., C47, 1077
Kutschera M., 1994, Phys. Lett. B, 340, 1
Levenfish K. P., Shibanov Yu. A., Yakovlev D. G., 1999, Astron. Lett., 25, 417
Lyne A. G., Pritchard R. S., Graham-Smith F., Camilo F., 1996, Nature, 381, 497
Meyer R. D., Pavlov G. G., Mészáros P., 1994, ApJ, 433, 265
Negele J. W., Vautherin D., 1973, Nucl. Phys., A207, 298
Ögelman H., Finley J. P., 1993, ApJ, 413, L31
Ögelman H., Finley J. P., Zimmerman H. U., 1993, Nature, 361, 136
Page D., Shibanov Yu. A., Zavlin V. E., 1996, in: Röntgenstrahlung from the Universe, eds. H. U. Zimmermann, J. Trümper, H. Yorke, MPE Report 263, p. 173; astro-ph/9601187
Pavlov G. G., Zavlin V. E., 1998, in: Neutron Stars and Pulsars, eds. N. Shibazaki, N. Kawai, S. Shibata, T. Kifune, p. 327
Possenti A., Mereghetti S., Colpi M., 1996, A&A, 313, 565
Potekhin A. Y., Chabrier G., Yakovlev D. G., 1997, A&A, 323, 415
Romani R. W., 1987, ApJ, 313, 718
Shibanov Yu. A., Zavlin V. E., Pavlov G. G., Ventura J., 1992, A&A, 266, 313
Wiringa R. B., Fiks V., Fabrocini A., 1988, Phys. Rev., C38, 1010